Evolution of Tropical and Extratropical Precipitation Anomalies During the 1997 to 1999 ENSO Cycle

By

Scott Curtis,
Joint Center for Earth Systems Technology
University of Maryland Baltimore County
Laboratory for Atmospheres
NASA/Goddard Flight Center
Code 912
Greenbelt, MD 20771 USA
curtis@agnes.gsfc.nasa.gov
phone: 301-614-6309
fax: 301-614-5492

Robert Adler,
Laboratory for Atmospheres
NASA/Goddard Flight Center

George Huffman, Eric Nelkin, and David Bolvin
Science Systems Applications Inc.
Laboratory for Atmospheres
NASA/Goddard Flight Center

97-98 ENSO

Abstract:

The 1997-1999 ENSO period was very powerful, but also well observed. Multiple satellite rainfall estimates combined with gauge observations allow for a quantitative analysis of precipitation anomalies in the tropics and elsewhere accompanying the 1997-99 ENSO cycle. An examination of the evolution of the El Niño and accompanying precipitation anomalies revealed that a dry Maritime Continent preceded the formation of positive SST anomalies in the eastern Pacific Ocean. 30-60 day oscillations in the winter of 1996/97 may have contributed to this lag relationship. Furthermore, westerly wind burst events may have maintained the drought over the Maritime Continent. The warming of the equatorial Pacific was then followed by an increase in convection. A rapid transition from El Niño to La Niña occurred in May 1998, but as early as October-November 1997 precipitation indices captured substantial changes in Pacific rainfall anomalies. The global precipitation patterns for this event were in good agreement with the strong consistent ENSO-related precipitation signals identified in earlier studies. Differences included a shift in precipitation anomalies over Africa during the 1997-98 El Niño and unusually wet conditions over northeast Australia during the later stages of the El Niño. Also, the typically wet region in the north tropical Pacific was mostly dry during the 1998-99 La Niña. Reanalysis precipitation was compared to observations during this time period and substantial differences were noted. In particular, the model had a bias towards positive precipitation anomalies and the magnitudes of the anomalies in the equatorial Pacific were small compared to the observations. Also, the evolution of the precipitation field, including the drying of the

Maritime Continent and eastward progression of rainfall in the equatorial Pacific, was less pronounced for the model compared to the observations.

KEYWORDS: ENSO, El Niño, La Niña, Precipitation, Tropics

1. Introduction

It can be argued that the 1997-98 El Niño was the strongest ENSO event ever recorded. The unusually warm waters of the equatorial Pacific were accompanied by changes in the large-scale circulation, followed by precipitation anomalies ranging from severe drought to floods. The Maritime Continent, Amazon and Congo basins, and Central America experienced drought during some part of 1997 and 1998, while Argentina, Peru, and East Africa were hardest hit by flooding. In fact, there have been many studies documenting the variability of regional precipitation during the 97-98 event (Montroy et al. 1998, Bell and Halpert 1998, Bell et al. 1999, Jaksic 1998, Mullen 1998, Pavia and Badan 1998, Harrison and Larkin 1998, Kogan 1998, Jensen et al. 1998, McPhadden 1999, Kousky 2000). The El Niño was followed by a persistent La Niña. The regional precipitation anomalies for this phase of the ENSO cycle have been less well documented.

Global precipitation during the 1997-99 ENSO was well observed from space. The SSM/I microwave and high resolution geo-IR data were available to monitor daily to monthly precipitation rates over even remote areas of the globe. The 1998-99 portion of the event was observed by the Tropical Rainfall Measuring Mission (TRMM) as discussed by Adler et al. (2000). In contrast, oceanic precipitation analyses for the comparable 1982-83 ENSO were limited to less capable satellite data, such as the outgoing longwave radiation information, or model data. With this motivation, satellite observations and gauges are used to examine the evolution of tropical and extratropical precipitation anomalies associated with the 1997-98 El Niño and 1998-99 La Niña. This work is intended to be a case study and the results found here may not be applicable to all

ENSO events. Finally, the observations will be compared to model generated precipitation during this period.

2. Data

The primary data source for this study is an experimental version of the monthly Global Precipitation Climatology Project's (GPCP; Huffman et al. 1997) community data set, hereafter referred to as GPCP. This data set is described by Huffman et al. (1997), except there has been a slight modification in the merger technique; it uses TOVS-based estimates of precipitation (Susskind et al. 1997) to fill in missing or uncertain data in the high latitudes, after being adjusted to GPCP values in nearby areas. The record is extended back before the SSM/I period using the OLR Precipitation Index (OPI) of Xie and Arkin (1998). The record of GPCP global monthly precipitation now extends from January 1979 to the present. The GPCP analysis has the distinctive feature of using the relatively infrequent low-orbit microwave observations to calibrate or adjust the geosynchronous IR-based estimates, thereby retaining the bias of the superior instantaneous rainfall observations and the superior sampling of the geosynchronous observations. GPCP is heavily weighted toward a gauge analysis over land (Rudolf et al. 1994). In general bimonthly averages of precipitation anomalies are shown, thereby reducing the effects of 30-60 day oscillations. However, individual months and twenty-year climatologies were examined as well.

GPCP is compared with NCEP/NCAR's reanalysis product (Kalnay et al. 1996). Precipitation is computed from a 62 wave triangular, 28 layer spectral model "Medium Range Forecast" run.

For the examination of smaller time and space scales, a one degree daily global precipitation data set (1DD; Huffman et al. 2000) was used. 1DD includes precipitation estimates from geosynchonous IR, and TOVS. 1DD is computed separately from the monthly GPCP analysis, but each day of the daily combination is scaled such that each month of daily data sums to the corresponding GPCP monthly estimate. This is done to ensure consistency between GPCP products and to introduce gauge data as a constraint on 1DD. The product currently extends from January 1997 to October 1999. NCEP/NCAR also produces a daily reanalysis precipitation data set, with zonal grid spacing of 1.875 °, and this was used to compare with the daily 1DD fields.

3. Evolution of Precipitation in the Tropics

3.1 Overview

This section presents a timeline of evolution of key components of the ocean-atmosphere system during the 1997-99 ENSO cycle. In particular, SST and precipitation anomalies are shown in Figs. 1 and 2. The beginning of 1997 saw a deep thermocline and warm ocean in the West Pacific and a shallow thermocline and cold ocean in the East Pacific (Bell and Halpert 1998). This was followed in early boreal spring by a rapid transition to El Niño conditions in the ocean. Anomalous warming in the east was accompanied by a flattening of the thermocline. A drying of the Maritime Continent preceded the SST increase in the east-central Pacific and the following increase in precipitation there. The anomalously dry conditions over the Maritime Continent and

warm waters over the central Pacific peaked at the end of 1997. The maximum precipitation anomaly in the Pacific followed in early 1998.

As the ENSO strengthened, changes were observed in the precipitation anomaly field in the central Pacific, which led the full onset of La Niña. A dipole of wet anomalies along the equator and dry anomalies to the north was consistent with an intensified meridional-vertical circulation (Curtis and Hastenrath 1997) from mid-1997 to mid-1998. The negative precipitation anomalies in the Pacific preceded the positive anomalies over the Maritime Continent. This change-over in the atmosphere coincided with rapid decreases in the SST and subsurface structure (Bell et al. 1999).

The SST and precipitation variability described above was quantified using indices over the Maritime Continent and Pacific basin. SST (Reynolds and Smith 1995) and precipitation anomalies were computed within a fixed box over the Maritime Continent (INDO; Fig. 3). Nino 3.4 (Fig. 3) was chosen to quantify SST anomalies in the east Pacific, and precipitation anomalies were calculated for this domain. Because of the varying nature of rainfall, moving boxes were also used to describe precipitation changes. Area averages of precipitation, the size of INDO and Nino 3.4, were moved throughout larger domains encompassing the Maritime Continent (MC) and east Pacific (P) (Fig. 3), as described by Curtis and Adler (2000). Here MC-(+) denotes the minimum (maximum) value in the moving block averages found within MC and P-(+) the minimum (maximum) value found within P. The same search procedure was used on anomalous precipitation (aMC-, aMC+, aP-, aP+), which should be related to anomalies in the vertical velocity field associated with the components of the Walker Circulation. Because these indices search for the largest anomalies in an area, they can often lead

fixed-location indices in detecting regional rainfall changes (Curtis and Adler 2000). An example of these moving box indices, aP+ and aMC-, is given in Fig. 4 (a reproduction of Fig. 2 in Curtis and Adler (2000)) for months during the 1997-98 El Niño. The normalized difference of aP+ minus aMC- is the El Niño Index (EI), a measure of the westward gradient of rainfall anomalies. The normalized difference of aMC+ minus aP- is the La Niña Index (LI), a measure of the opposite, eastward gradient of rainfall anomalies. The El Niño Index minus the La Niña Index yields the ENSO Precipitation Index (ESPI). The EI,LI, and ESPI are related to the anomalous strength of the Walker Circulation, and are correlated well with traditional ENSO indices, such as Nino 3.4 and the Southern Oscialltion Index (SOI). Time series plots from 1996 to 1998 are shown in Fig. 5 for Nino 3.4 (sst, precipitation), INDO (sst, precipitation), aMC+, aMC-, aP+, aP-, and Fig. 6 for EI, LI, and ESPI.

3.2 Initiation of El Niño

The period of initiation and intensification of the El Niño was roughly January to December 1997 (see bold lines in Figs. 5 and 6). Prior to that, the climate system was in the La Niña phase. It was the fourth strongest La Niña according to over 20 years of ESPI data, but relatively weak compared to the long-term SST and SOI records. Early indications of a change in the climate system were seen through decreases in precipitation averages over the Maritime Continent (Fig. 5b,c) in September-October 1996. During November-December 1996 (Fig. 1a,b) the Maritime Continent was generally wet, and the central Pacific dry. However, an area of negative precipitation anomalies is found over Indonesia and Borneo, which is consistent with negative aMC- and INDO(precipitation)

values for this period (Fig. 5b,c). In January-February 1997 (Fig. 1d) the dry region over the eastern equatorial Indian Ocean and Indonesia intensified. Nino 3.4(sst) became positive in March 1997 (Fig. 5a). In fact, of the standard equatorial Pacific SST indices, only Nino 4 (5 °N - 5 °S; 160 °E - 150 °W) showed a concurrent evolution to positive values as compared to aMC- and INDO(precipitation). The Madden-Julian Oscillation (MJO) may have influenced the decrease in precipitation over the Maritime Continent before the appearance of El Niño SSTs. Fig. 7 shows a global time-longitude diagram of daily precipitation averaged from 5° N to 5° S using the global, daily analysis of Huffman et al. (2000) (see section 2). The period is January 1 1997 to December 31 1998. An active MJO is apparent from 140E to 160W for most of 1997.

In March-April 1997 a warm anomaly emerged off the coast of Peru (Fig. 1e). In the East Pacific the climatological weaker band of precipitation south of the equator was absent, while in the West Pacific the ITCZ and South Pacific Convergence Zone (SPCZ) were further apart than normal. This pattern of precipitation was consistent with negative precipitation anomalies over the Maritime Continent, extending eastward in a band along the equator and positive rainfall anomalies located immediately to the north and south (Fig. 1f). The clearing along the equator (shown from November 1996 to April 1997) may have contributed, through increased short wave radiation, to an intensification of the warming of the equatorial cold tongue in this case. This is consistent with Weare (1983) who hypothesized that increased surface heating plays a role in the early stages of a developing El Niño. However, further investigation of the role of clouds in the initiation of the 1997-98 El Niño is needed. In any event, warm El Niño waters had extended into the central Pacific by May-June 1997 (Fig. 1g). At the same time the rain band

accompanying the ITCZ had begun to broaden, intensify, and migrate southward, consistent with a weakening of the Walker circulation. Interestingly, the precipitation and SST signals were not co-located. The increase in rainfall occurred in the central basin just off the equator (Fig. 1h), and the warm anomalies covered the equatorial cold tongue in the east (Fig. 1g). The warming (Fig 1i), in turn, provided the energy for abnormal convection in the Nino 3.4 region (Fig. 1j). This is borne out in Fig. 5a and b, as Nino 3.4(sst) leads Nino 3.4(precipitation). This apparent thermodynamic relation does not hold true in the Maritime Continent, where a decrease in INDO(precipitation) occurs well before a small decrease in INDO(sst) (Fig. 5a,b).

The second half of 1997 saw an enhanced warming of the east-central Pacific and continued weakening of the Walker Circulation. Elsewhere in the tropics, a delayed onset of the Asian monsoon (as indicated by Fig. 1h) was followed by both positive and negative precipitation anomalies over the Indian subcontinent in July-August 1997 (Fig. 1j). By September-October 1997 (Fig. 1k ,l) there was a decrease in convection over the Congo and Amazon basins. Finally, an increase in rainfall over east Africa coincided with a warming of the Indian Ocean from September-October to November-December (Fig. 1k,l,m,n).

Fig. 1 clearly shows that the negative precipitation anomalies over the Maritime Continent in November-December 1997 can be traced back a whole year, while the El Niño SST signal in the east-central Pacific can be traced back to March-April. During this time the MJO was active in the western Pacific. Also, the drying of the Maritime Continent went through two periods of intensification, namely from January-February to March-April, and from July-August to September-October (Fig. 1). It appears that these

changes may have taken place on the order of days. Fig. 8 shows the MC- index of precipitation for 1997. A 30 day running mean of MC- is step-like, with the largest decreases occurring from January to March. A lesser decrease occurred in July. Three days in February-March are shown in map form. During the precipitous drop in MC- from a maximum on February 20 to a minimum on March 2 the heaviest precipitation moved eastward off the Maritime Continent. This movement of the convection coincides with a westerly wind burst event documented by Yu and Rienecker (1998).

3.3 Mature Phase and Transition to La Niña

The temperature anomalies in the east-central Pacific reached a maximum in November-December 1997 (Fig. 1m). Nino 1+2, 3, 3.4, and 4 all show a maximum in either November or December. Precipitation within the SPCZ and Pacific ITCZ merged, forming a region of positive precipitation anomaly east of the date line (Fig. 3n). The maximum in Nino 3.4(precipitation) in December-January (Fig. 5b) followed the maximum in Nino 3.4(sst) in November (Fig. 5a). The largest precipitation anomalies in the Pacific, as quantified by aP+ (Fig. 5c), occurred even later during January-February 1998 (Fig. 4a,b) after SST anomalies began to decline. However, the actual SSTs during this period remained near 29C and the atmosphere and ocean remained highly coupled (a manifestation of continuing mature phase ENSO conditions) as evidenced by abnormally active convection. This decline in SST anomalies occurred because the climatological mean SST increased as January-February begins the march toward increasing SST in the east Pacific (which peaks in April-May). As measures of the gradient of precipitation, both EI and ESPI peaked in September-October 1997 (Fig. 6), slightly leading the Nino

3.4 averages (Fig. 5a,b), and somewhat before the occurrence of the largest precipitation anomalies in the Pacific (Fig. 5c). According to the EI and ESPI the 1997-98 El Niño event was the strongest over the past 20 years (Curtis and Adler 2000).

During the maturation of the El Niño, in September-October 1997, aMC+ and aP- began to rise and fall respectively (Fig. 5d), continuing into the La Niña phase. The largest dry anomalies in the Pacific (aP-) were found north of the enhanced rainfall in September-October (Fig. 1l) and November-December (Fig. 1n) and northwest in January-February (Fig. 2b) and March-April (Fig. 2d) where aP- peaked at -7 mm day^{-1} (Fig. 5d). At the same time the positive precipitation anomalies in the eastern Pacific had weakened slightly (Fig. 2d). Above normal rainfall was observed over New Guinea in November-December 1997 (Fig. 1n), spreading throughout the Maritime Continent by March-April 1998 (Fig. 2d). Also during this season, Northeast Brazil was anomalously dry but the Maritime Continent drought had begun to end. A weak El Niño (in terms of SST anomalies) in May-June 1998 was accompanied by mostly negative precipitation anomalies in the Pacific (Fig. 2e, f). However, rainfall anomalies in excess of 10 mm day^{-1} remained off the coast of Peru. During May 1998 a precipitation complex traveled from the east coast of Africa to the eastern Pacific in a matter of days during the rapid decay of El Niño and initiation of La Niña. Takayabu et al. (1997) suggest that an MJO influenced the termination of El Niño through the intensification of easterly trade winds. By July-August 1998 the SST pattern in the Pacific was more characteristic of a La Niña than an El Niño. The Walker circulation continued to strengthen as positive precipitation anomalies covered the East Indian Ocean and western Maritime Continent and negative anomalies dominated the western equatorial Pacific (Fig. 2g, h).

From September-October 1998 to January-February 1999 (Figs. 2i,j,k,l,m,n) a steep gradient of anomalous precipitation was formed in the western Pacific, as the convection center of the Maritime Continent and SPCZ continued to intensify and the largest negative precipitation anomalies shifted westward. In January-February 1999 (Fig. 2m,n) enhanced rainfall was observed over the Amazon basin and southeastern Africa, while the Indian Ocean and equatorial Africa were covered by dry anomalies. The La Niña persisted from spring 1999 through spring 2000 (not shown).

4. Global Patterns of Normalized Precipitation Anomalies

The precipitation anomalies accompanying the 97-99 ENSO are illustrated by six month seasons of normalized values (Figs. 9 and 10). These maps are then compared with schematic diagrams from the landmark studies of Ropelewski and Halpert (1987, 1989; hereafter referred to as RH). The solid (dashed) line areas are consistently dry (wet) for ENSO events during the past century. April 1997 to September 1997 (Fig. 9a) would correspond to Apr(0) - Sep(0) in RH's notation of seasons of maximum sensitivity (Fig. 9c). According to RH, during these early months northern India, the Maritime Continent, southeast Australia, and northern South America are typically dry, while the western U.S. is wet (Fig. 9c). 1997 follows this pattern according to GPCP. However, the interior of India was more wet than dry (Fig. 9a). In the October(0) to March(+) season there is also good agreement between the typical global precipitation signal and this case study. Some exceptions for 1997-98 are noted. The dipole of precipitation anomalies over Africa (Fig. 9c) is shifted (Fig. 9b) and northeast Australia, which

averaged dry from April(0) to September(0) (Fig. 9a), averaged wet from October(0) to March(+) (Fig. 9b). GPCP also shows substantial rainfall anomalies over the oceans. For example, it was significantly wet from the coast of China eastward and significantly dry about the Drake Passage (Fig. 9b). RH captures the anomalous rains of the central Pacific (Fig. 9c) but not the statistically significant anomalies of the East Pacific (Fig. 9b).

Fig. 10 continues the ENSO into the La Niña phase. April to September 1998 shows a combination of El Niño and La Niña signals (Fig. 10a). RH depicts wet conditions over India in this season, while the normalized anomalies for this event are weakly negative. The months October 1998 to March 1999 (Fig. 10b) closely match the seasons chosen by RH to classify the canonical La Niña signals (Fig. 10c). The wet and dry regions during a typical La Niña are reproduced well with the 1998-99 case. However, in the historic composite the area to the north of the equator, encompassing Hawaii, is wet during November(0) to April(+) (Fig. 10c), while a much smaller area, which does not include Hawaii, is wet from October 1998 to March 1999 (Fig. 10b). The global map of satellite observations also shows dry conditions over the Indian Ocean for La Niña, and wet conditions in the Drake Passage (Fig. 10b). In fact, the precipitation anomalies for the 1997-98 El Niño are inverse to the 1998-99 La Niña for many regions of the tropics and extratropics. Unlike the typical ENSO cycle, the La Niña has persisted through 1999 and into 2000.

5. Observed Versus Modeled Precipitation

The evolution of NCEP/NCAR reanalysis derived precipitation shows some striking differences from the observations. The absolute magnitudes of the modeled NINO 3.4 and INDO precipitation anomalies are smaller than observed (Fig. 11a). For GPCP, INDO reached a minimum well before the NINO 3.4 precipitation anomaly reached a maximum. However, the model shows a simultaneous peak in the indices (Fig. 11a). The extremes of aP+ and aMC- associated with the El Niño occurred nearly six months earlier for the reanalysis than for the observations (Fig. 11b). Finally, the time series plots of aMC+ and aP- are different for GPCP as compared to NCEP/NCAR, especially in 1997 when the observations show the beginnings and evolution of the La Niña pattern from November 1997 onward, whereas the modeled precipitation fails to capture these rapid changes (Fig. 11c).

Fig. 12 shows the April 1997 to March 1998 average for GPCP, NCEP/NCAR, and the GPCP minus NCEP/NCAR difference. Although the ENSO signal is present in the modeled precipitation anomalies, there are substantial differences in magnitude between the reanalysis and observed estimates. As noted in a recent study by Janowiak et al. (1998) comparing GPCP and NCEP/NCAR, the magnitudes of the reanalysis values are smaller than those observed on the interannual time scale. In the central Pacific only a small area of modeled precipitation anomalies is greater than 4 mm day^{-1} and none of the anomalies in the Maritime Continent are less than –4 mm day^{-1} (Fig. 12b). In fact, the maximum anomalous precipitation rate within the wet equatorial East Pacific is 7.7 mm day^{-1} for the observations as compared to 5.4 mm day^{-1} for the model, while the minimum

anomalous precipitation rate over the Maritime Continent is -6.1 and -4.0 mm day^{-1} respectively. The NCEP/NCAR average map shows very wet anomalies over India and very dry anomalies over equatorial South America which were not observed (Fig. 12). Also, NCEP/NCAR anomalies tend to be predominantly positive (Janowiak et al. 1998).

A similar Hovmöller analysis as presented in Fig. 7 was performed on the NCEP/NCAR data (not shown here). Globally, magnitudes of the modeled precipitation were smaller than those observed. The observations (Fig. 7) suggest that equatorial mesoscale complexes are an important mechanism for the propogation of substantial rainfall amounts from the Maritime Continent to the East Pacific. However, in the reanalysis these systems are less well defined and there seems to be a large scale spreading of light precipitation across the basin. In fact, in early 1998 the model shows about equal precipitation amounts in the East and West Pacific. Finally, the NCEP/NCAR reanalysis incorrectly produced continuous convective precipitation between 90° and 120° E during 1997-98, which is consistent with the model-based small negative anomalies over the Maritime Continent in Fig. 12b. This inaccuracy in resolving the convectively coupled equatorial waves may be a reason why the model does not show propagation of positive precipitation anomalies to the East Pacific in early 1998, and produces only a weak anomalous precipitation gradient in the Pacific basin during the ENSO.

6. Conclusions

This work was a contribution to the understanding of the evolution of precipitation patterns during the 1997-99 ENSO cycle. Monthly and daily GPCP precipitation data sets were used to monitor the evolution of tropical and extratropical precipitation during the 1997-98 El Niño and beginning of the 1998-99 La Niña. Comparisons were made with NCEP/NCAR model output.

The evolution of the ENSO was tracked by maps of SST and precipitation anomalies and quantified by a suite of indices in the Pacific basin and Maritime Continent. The data suggests that at the beginning of the event in the winter of 1996/97 30-60 day oscillations may have influenced a climatological drying of the Maritime Continent as clouds and precipitation were advected eastward. A month or two later there was a warming of the east-central Pacific which contributed to enhanced convection. It was shown that westerly wind burst events were associated with a rapid movement of precipitation eastward from the Maritime Continent to the West Pacific and that less precipitation returned after the event was over, leading to a step-down drying the Maritime Continent. Two of these decreases in rainfall occurred in late February and July. The precipitation-based El Niño Index indicated that the gradient of precipitation anomalies in the Pacific (positive in the east and negative in the west) was a maximum during September-October 1997, before the peak in Nino 3.4 SST anomalies in November 1997. At the same time the La Niña Index turned upwards, capturing negative precipitation anomalies to the north of the equator. The rapid transition from El Niño to La Niña in May 1998 was indicated by concurrent changes in precipitation and SST.

Global patterns of precipitation anomalies during these years were in general consistent with the typical ENSO patterns described in previous studies. Differences included a shift in precipitation anomalies over Africa during the 1997-98 El Niño and unusually wet conditions over northeast Australia during the later stages of the El Niño. Also, the typically wet region to the north of the equator in the Pacific was mostly dry during the 1998-99 La Niña. The precipitation observations revealed strong precipitation anomalies over the Indian Ocean, southeast Pacific basin, North Atlantic, and other areas not well observed with surface data.

There were several discrepancies between the observed precipitation anomalies and those computed by the NCEP/NCAR model during 1997-98. The reanalysis product has a bias towards positive precipitation anomalies and the magnitudes of the anomalies in the equatorial Pacific were small as compared to the observations. The evolution of the event was also different for the model. During the onset of the El Niño the model decrease in precipitation over the Maritime Continent occurred simultaneously with the increase in precipitation in the East Pacific, unlike the observations where the Maritime Continent drying occurred first. Also, the transition from El Niño to La Niña was not as abrupt. The MJO was resolved by NCEP/NCAR, but not the westerly wind bursts. This may have contributed to the model producing weaker negative precipitation anomalies in the west Pacific and weaker positive precipitation anomalies in the east Pacific as compared to the observations.

Future work will focus on using the 20 years of precipitation data to relate the pattern of evolution of the 1997-98 El Niño and 1998-99 La Niña to other ENSO events.

Acknowledgements: Special thanks go to John Janowiak for his insightful comments and for providing the monthly gridded NCEP precipitation data. This research is supported through the TRMM Science Team and NASA's Atmospheric Dynamics and Thermodynamics Program under Dr. Ramesh Kakar.

Figure Captions

Fig. 1. Bimonthly averages of SST (a, c, e, g, i, k, m) and precipitation (b, d, f, h, j, l, n) anomalies in C degrees and mm day-1 respectively, from November 1996 to December 1997. (a) SST November-December 1996 (Nov-Dec 96), (b) Precipitation Nov-Dec 96, (c) SST January-February 1997 (Jan-Feb 97), (d) Precipitation Jan-Feb 97, (e) SST March-April 1997 (Mar-Apr 97), (f) Precipitation Mar-Apr 97, (g) SST May-June 1997 (May-Jun 97), (h) Precipitation May-Jun 97, (i) SST July-August 1997 (Jul-Aug 97), (j) Precipitation Jul-Aug 97, (k) SST September-October 1997 (Sep-Oct 97), (l) Precipitation Sep-Oct 97, (m) SST November-December 1997 (Nov-Dec 97), (n) Precipitation Nov-Dec 97.

Fig. 2. Same as Fig. 3; period from January 1998 to February 1999. (a) SST January-February 1998 (Jan-Feb 98), (b) Precipitation Jan-Feb 98, (c) SST March-April 1998 (Mar-Apr 98), (d) Precipitation Mar-Apr 98, (e) SST May-June 1998 (May-Jun 98), (f) Precipitation May-Jun 98, (g) SST July-August 1998 (Jul-Aug 98), (h) Precipitation Jul-Aug 98, (i) SST September-October 1998 (Sep-Oct 98), (j) Precipitation Sep-Oct 98, (k) SST November-December 1998 (Nov-Dec 98), (l) Precipitation Nov-Dec 98, (m) SST January-February 1999 (Jan-Feb 99), (n) Precipitation Jan-Feb 99.

Fig. 3. Areas represented by indices. The large solid-lined and dashed-lined boxes indicate the Pacific (P) and Maritime Continent (MC) regions respectively. Shaded regions mark the locations of INDO (5N, 5S; 90E, 140E) and NINO 3.4 (5N, 5S; 170W, 120W) and represent the areas over which aMC and aP are computed.

Fig. 4. Reproduction of Figure 2 in Curtis and Adler (2000). GPCP derived rainfall anomalies in mm day^{-1}. Boxed regions are as in Fig. 1. The solid-lined box within P is the area with the maximum averaged precipitation anomaly (aP+) and the dashed-lined box within MC is the area with the minimum averaged precipitation anomaly (aMC-). (a) August 1997, (b) October 1997, (c) December 1997, (d) February 1998.

Fig. 5. 1996-98 time series of monthly sea surface temperature (SST) and bi-monthly precipitation indices for the central Pacific and Maritime Continent (ref. Fig. 1). Vertical lines denote Januarys. Bi-monthly values are plotted between month tick marks. For panels (a)-(c) thick lines connect the zero points to the maximum anomalies during the 97-98 El Niño. For panel (d) thick lines connect the zero points to the ends of the plots. (a) Solid line tracks Nino 3.4 (5N-5S, 170W-120W) and dashed line the INDO SST index (5N-5S, 90E-140E). (b) Solid and dashed lines track observed precipitation anomalies averaged over the Nino 3.4 and INDO areas respectively. (c) Solid and dashed lines denote observed aP+ and aMC- precipitation indices respectively. (d) Solid and dashed lines denote observed aMC+ and aP- precipitation indices respectively.

Fig. 6. 1996-98 time series of bi-monthly indices of anomalous precipitation gradient in the equatorial Pacific. Vertical lines denote Januarys. Bi-monthly values are plotted between month tick marks. Solid line tracks the ENSO Precipitation Index (ESPI), short-dased line El Niño Index (EI), and long-dashed line La Niña Index (LI). Thick lines connect the zero points to the maximum anomalies during the 97-98 El Niño.

Fig. 7. Time-longitude diagram (5° N to 5° S) of global precipitation derived from an experimental one degree daily product. Period is January 1 1997 to December 31 1998. Color bar denotes precipitation rates from 0 to 20 mm day^{-1}.

Fig. 8. Experimental one degree daily precipitation during a westerly wind burst event in late February 1997. MC- is plotted in mm day-1 for 1997 and during the period February 10 to March 10. Thick line in top panel is 30-day running mean. Precipitation fields are shown for February 22, February 26, and March 4, where shading is delineated every 5 mm day^{-1}. Black denotes rain rates in excess of 5 mm day^{-1}, white rain rates in excess of 25 mm day^{-1}.

Fig. 9. Six month seasons of normalized precipitation anomalies during the El Niño. Top panel is for April to September 1997 and middle panel is for October 1997 to March 1998. Bottom panel is a reproduction of Fig. 21 in Ropelewski and Halpert (1987). Dashed lines denote typically wet and solid lines dry regions in the seasons indicated. Year zero would correspond to 1997.

Fig. 10. Same as Fig. 9, but during the La Niña. Top panel is for April 1998 to September 1998 and middle panel is for October 1998 to March 1999. Bottom panel is a reproduction of Fig. 18 in Ropelewski and Halpert (1989). Dashed lines denote typically wet and solid lines dry regions in the seasons indicated. Year zero would correspond to 1998.

Fig. 11. 1996-98 time series of indices described in Fig. 5 derived from both observation (thin lines) and model (thick lines). Vertical lines denote Januarys. Bi-monthly values are plotted between month tick marks. (a) Solid and dashed lines track precipitation anomalies averaged over the Nino 3.4 and INDO areas respectively. (b) Solid and dashed lines denote aP+ and aMC- precipitation indices respectively. (c) Solid and dashed lines denote aMC+ and aP- precipitation indices respectively.

Fig. 12. Precipitation anomalies averaged for the year April 1997 to March 1998. Base period is 1987-96. Shading denotes positive values. Spacing is 2 mm day^{-1}.
(a) GPCPx, (b) NCEP/NCAR, (c) the difference GPCPx minus NCEP/NCAR.

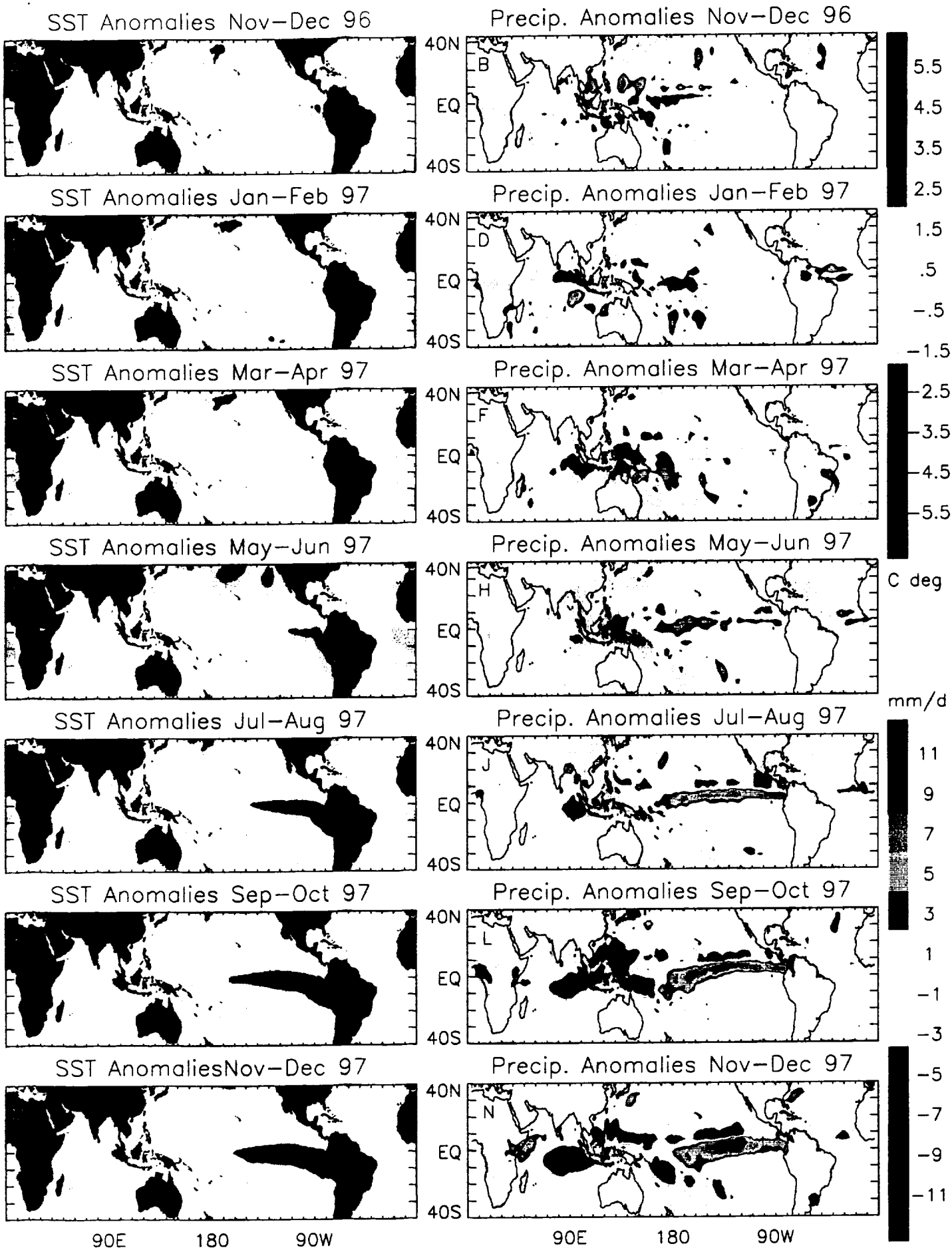
SST Anomalies Nov–Dec 96
Precip. Anomalies Nov–Dec 96
B
SST Anomalies Jan–Feb 97
Precip. Anomalies Jan–Feb 97
D
SST Anomalies Mar–Apr 97
Precip. Anomalies Mar–Apr 97
F
SST Anomalies May–Jun 97
Precip. Anomalies May–Jun 97
H
SST Anomalies Jul–Aug 97
Precip. Anomalies Jul–Aug 97
J
SST Anomalies Sep–Oct 97
Precip. Anomalies Sep–Oct 97
L
SST AnomaliesNov–Dec 97
Precip. Anomalies Nov–Dec 97
N
40N
EQ
40S
90E
180
90W
5.5
4.5
3.5
2.5
1.5
.5
−.5
−1.5
−2.5
−3.5
−4.5
−5.5
C deg
mm/d
11
9
7
5
3
1
−1
−3
−5
−7
−9
−11

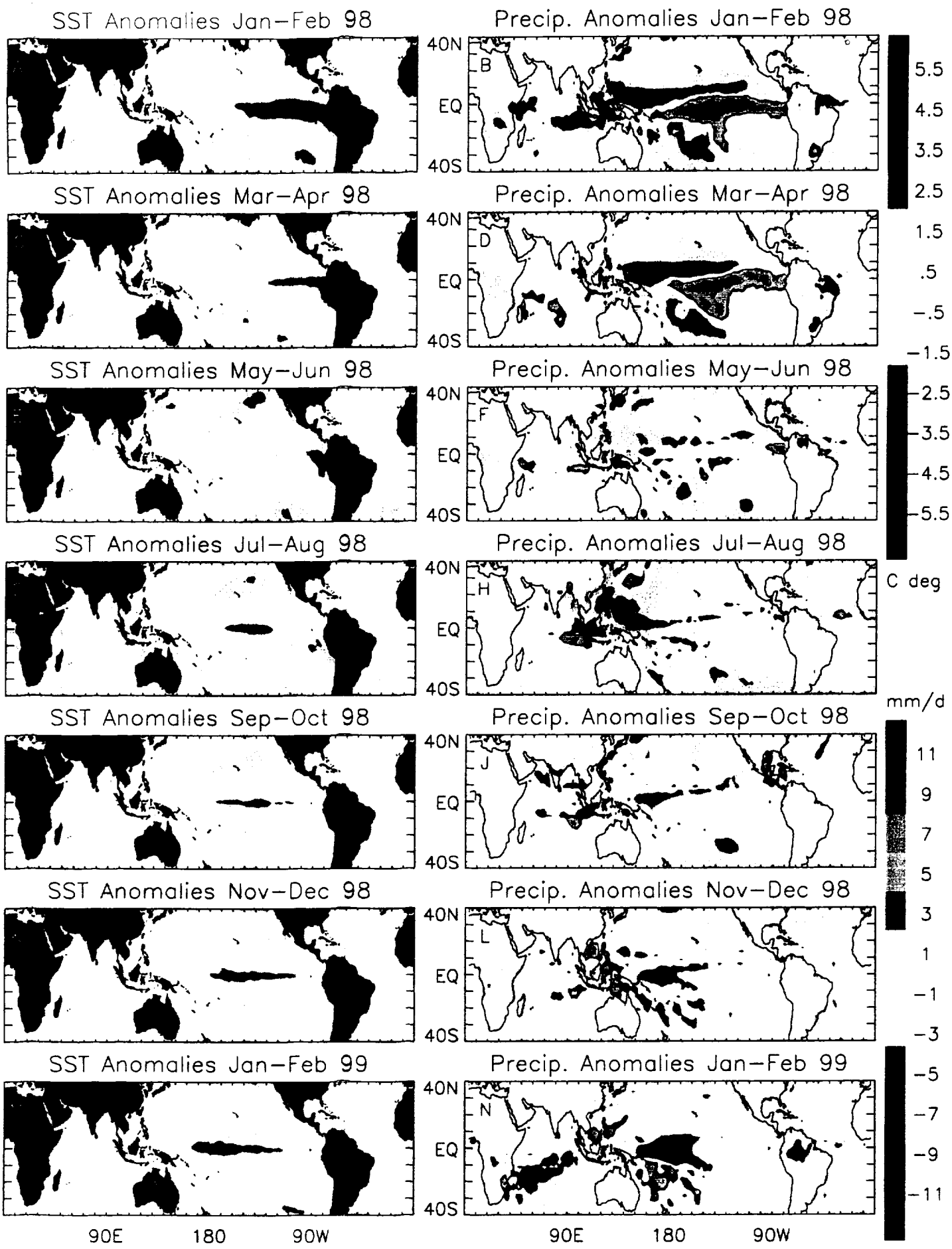
SST Anomalies Jan–Feb 98
Precip. Anomalies Jan–Feb 98
B
SST Anomalies Mar–Apr 98
Precip. Anomalies Mar–Apr 98
D
SST Anomalies May–Jun 98
Precip. Anomalies May–Jun 98
F
SST Anomalies Jul–Aug 98
Precip. Anomalies Jul–Aug 98
H
SST Anomalies Sep–Oct 98
Precip. Anomalies Sep–Oct 98
J
SST Anomalies Nov–Dec 98
Precip. Anomalies Nov–Dec 98
L
SST Anomalies Jan–Feb 99
Precip. Anomalies Jan–Feb 99
N
40N
EQ
40S
90E
180
90W
5.5
4.5
3.5
2.5
1.5
.5
−.5
−1.5
−2.5
−3.5
−4.5
−5.5
C deg
mm/d
11
9
7
5
3
1
−1
−3
−5
−7
−9
−11

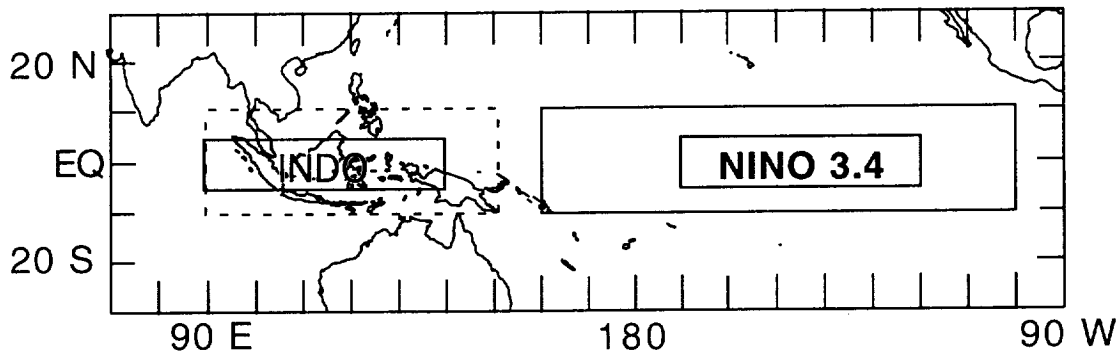
20 N
EQ
20 S
INDO
NINO 3.4
90 E
180
90 W

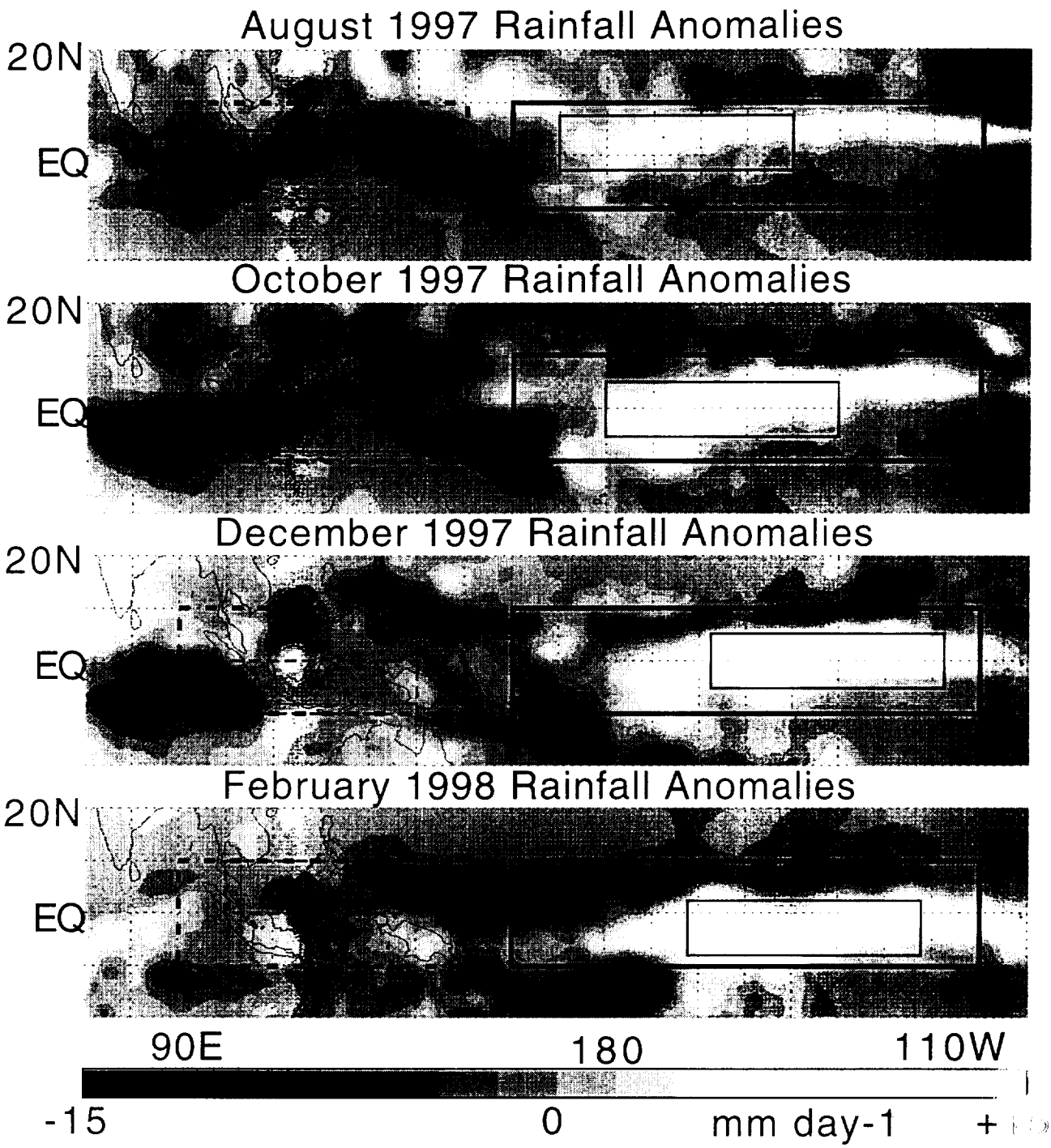
August 1997 Rainfall Anomalies
20N
EQ
October 1997 Rainfall Anomalies
20N
EQ
December 1997 Rainfall Anomalies
20N
EQ
February 1998 Rainfall Anomalies
20N
EQ
90E
180
110W
-15
0
mm day-1
+

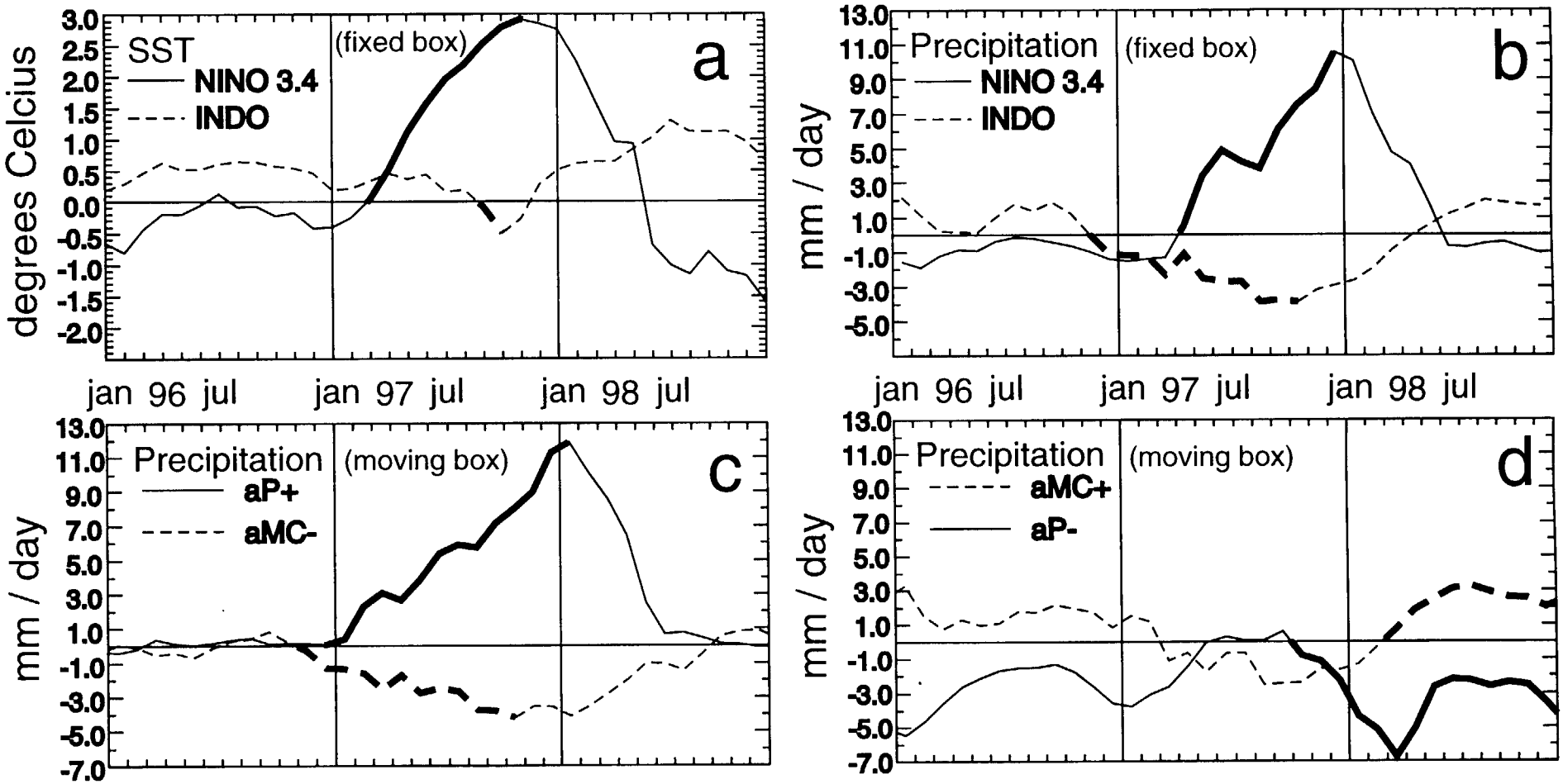
degrees Celcius
SST
NINO 3.4
INDO
(fixed box)
a
3.0
2.5
2.0
1.5
1.0
0.5
0.0
-0.5
-1.0
-1.5
-2.0
jan 96 jul
jan 97 jul
jan 98 jul
mm / day
Precipitation
NINO 3.4
INDO
(fixed box)
b
13.0
11.0
9.0
7.0
5.0
3.0
1.0
-1.0
-3.0
-5.0
jan 96 jul
jan 97 jul
jan 98 jul
mm / day
Precipitation
aP+
aMC-
(moving box)
c
13.0
11.0
9.0
7.0
5.0
3.0
1.0
-1.0
-3.0
-5.0
-7.0
mm / day
Precipitation
aMC+
aP-
(moving box)
d
13.0
11.0
9.0
7.0
5.0
3.0
1.0
-1.0
-3.0
-5.0
-7.0

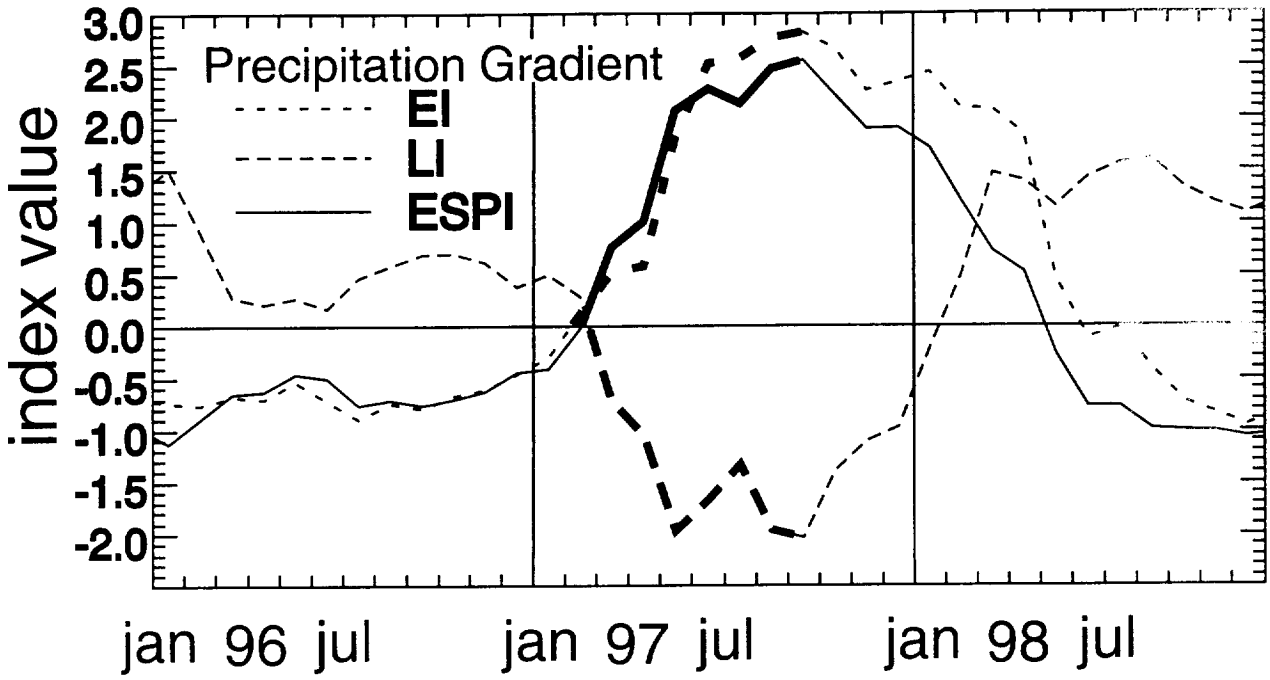
Precipitation Gradient
EI
LI
ESPI
index value
3.0
2.5
2.0
1.5
1.0
0.5
0.0
-0.5
-1.0
-1.5
-2.0
jan 96 jul
jan 97 jul
jan 98 jul

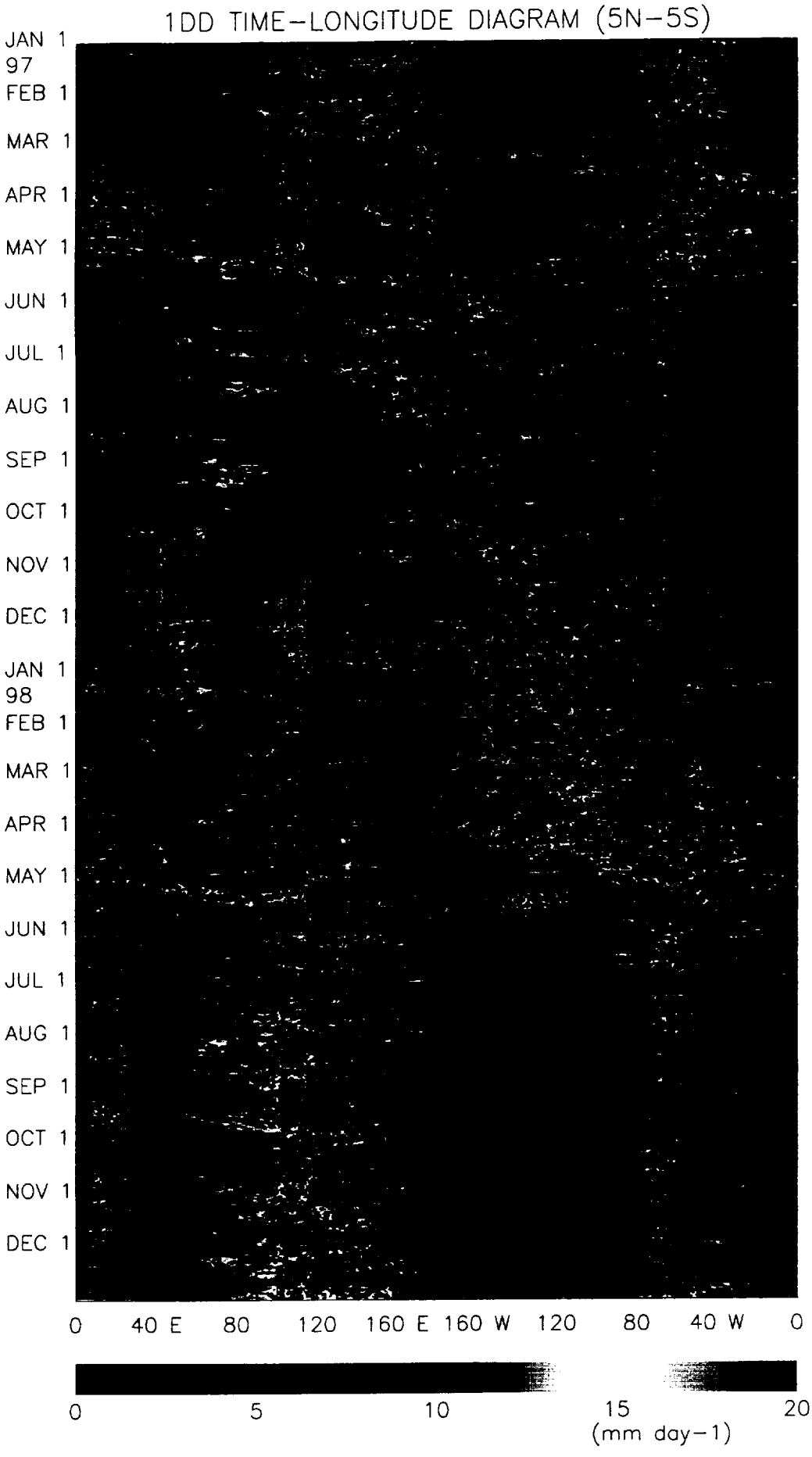
1DD TIME-LONGITUDE DIAGRAM (5N-5S)
JAN 1
97
FEB 1
MAR 1
APR 1
MAY 1
JUN 1
JUL 1
AUG 1
SEP 1
OCT 1
NOV 1
DEC 1
JAN 1
98
FEB 1
MAR 1
APR 1
MAY 1
JUN 1
JUL 1
AUG 1
SEP 1
OCT 1
NOV 1
DEC 1
0
40 E
80
120
160 E
160 W
120
80
40 W
0
0
5
10
15
20
(mm day-1)

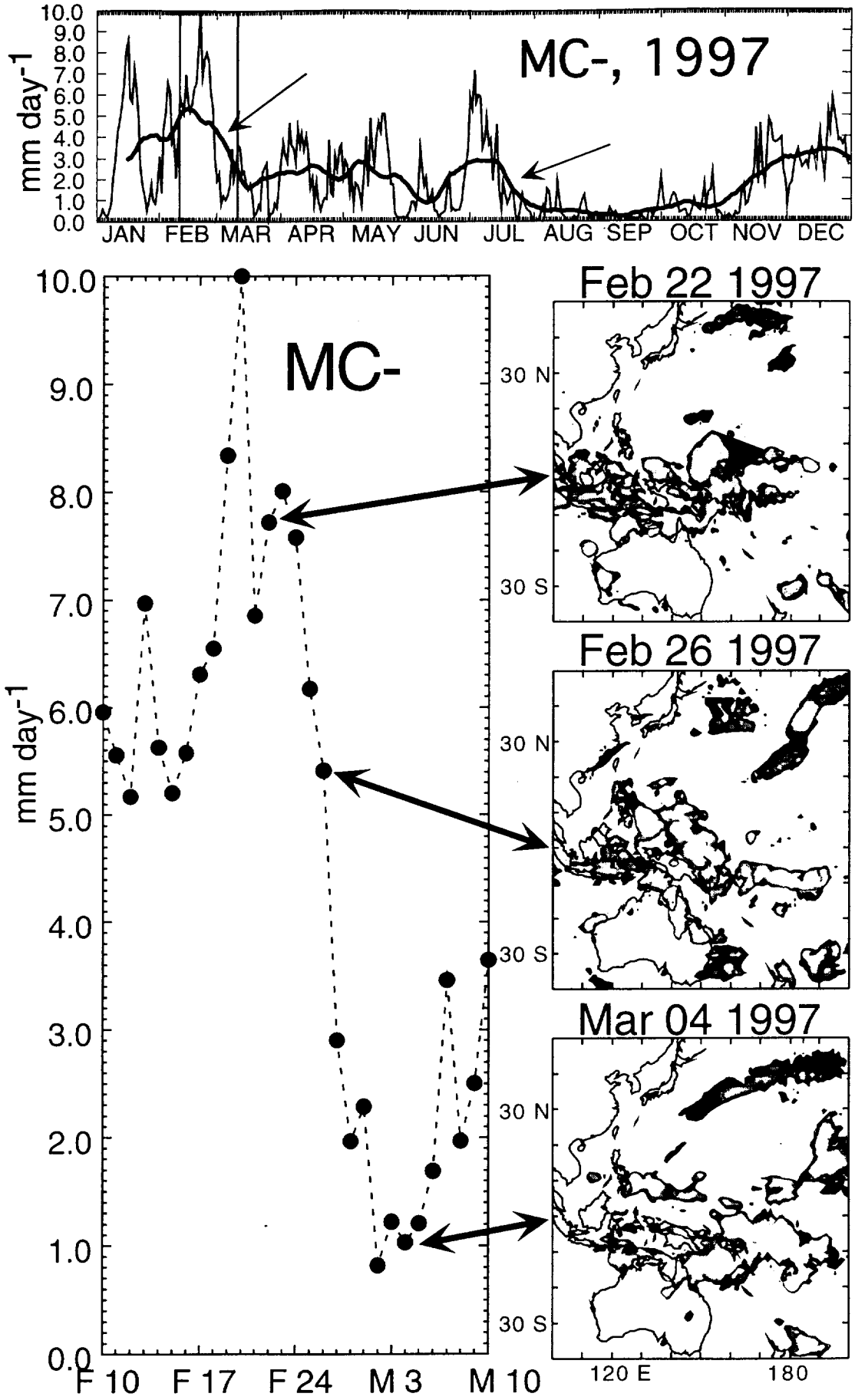
MC-, 1997
mm day-1
10.0
9.0
8.0
7.0
6.0
5.0
4.0
3.0
2.0
1.0
0.0
JAN FEB MAR APR MAY JUN JUL AUG SEP OCT NOV DEC
MC-
Feb 22 1997
Feb 26 1997
Mar 04 1997
30 N
30 S
F 10 F 17 F 24 M 3 M 10
120 E
180

April(0) 1997 to September(0) 1997

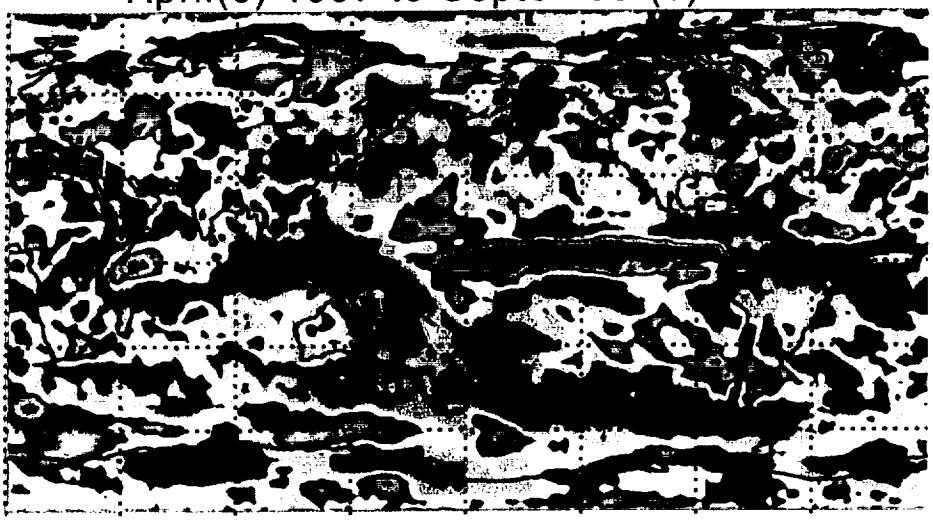

October(0) 1997 to March(+) 1998

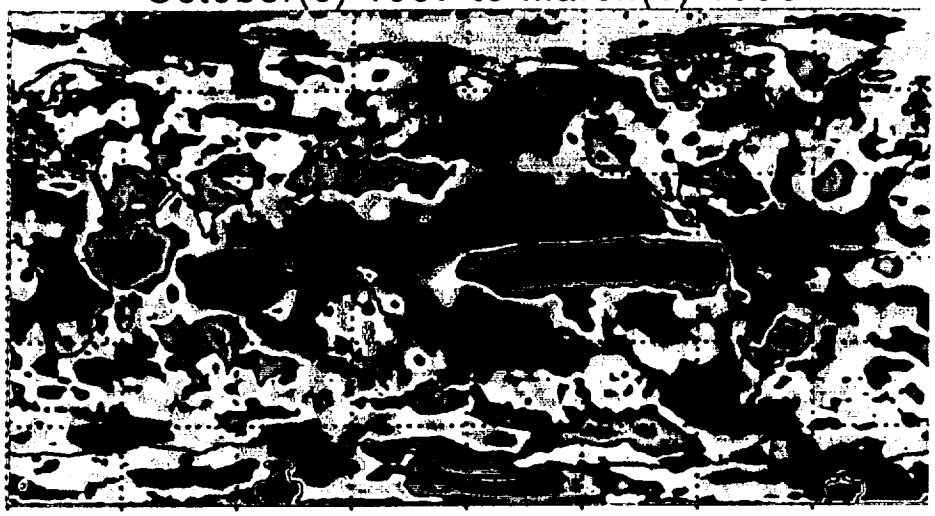

Ropelewski and Halpert (El Niño)

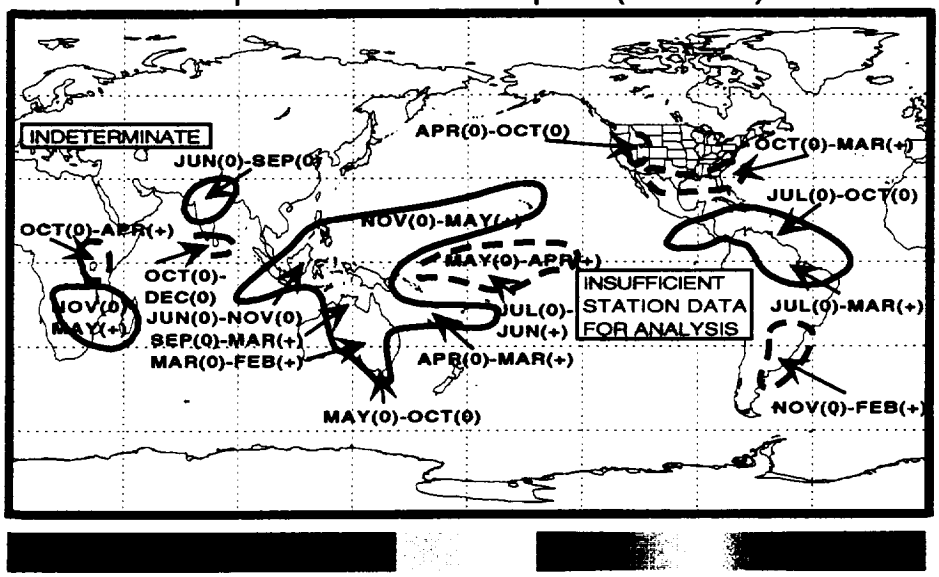

−2.0 0.0 2.0

April(0) 1998 to September(0) 1998

October(0) 1998 to March(+) 1999

Ropelewski and Halpert (La Niña)

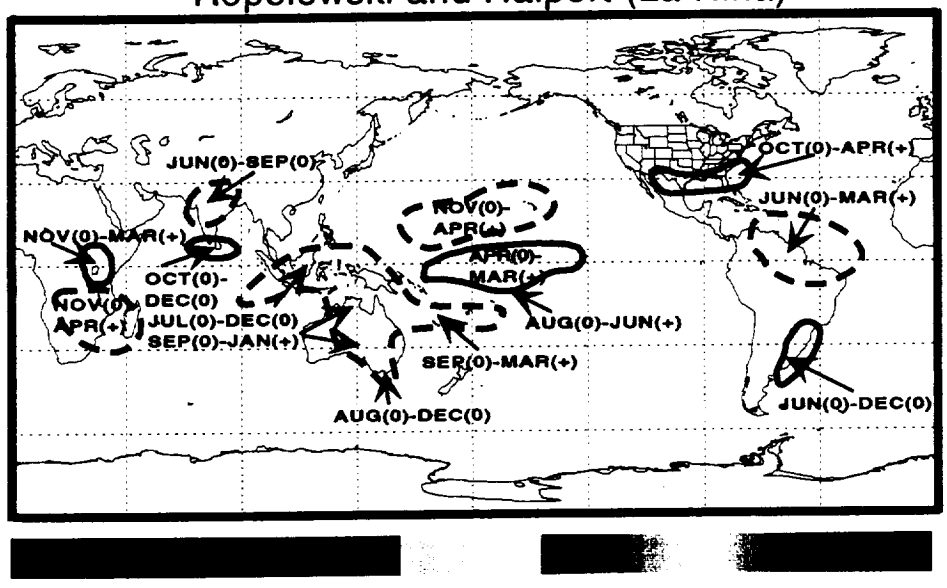

−2.0 0.0 2.0

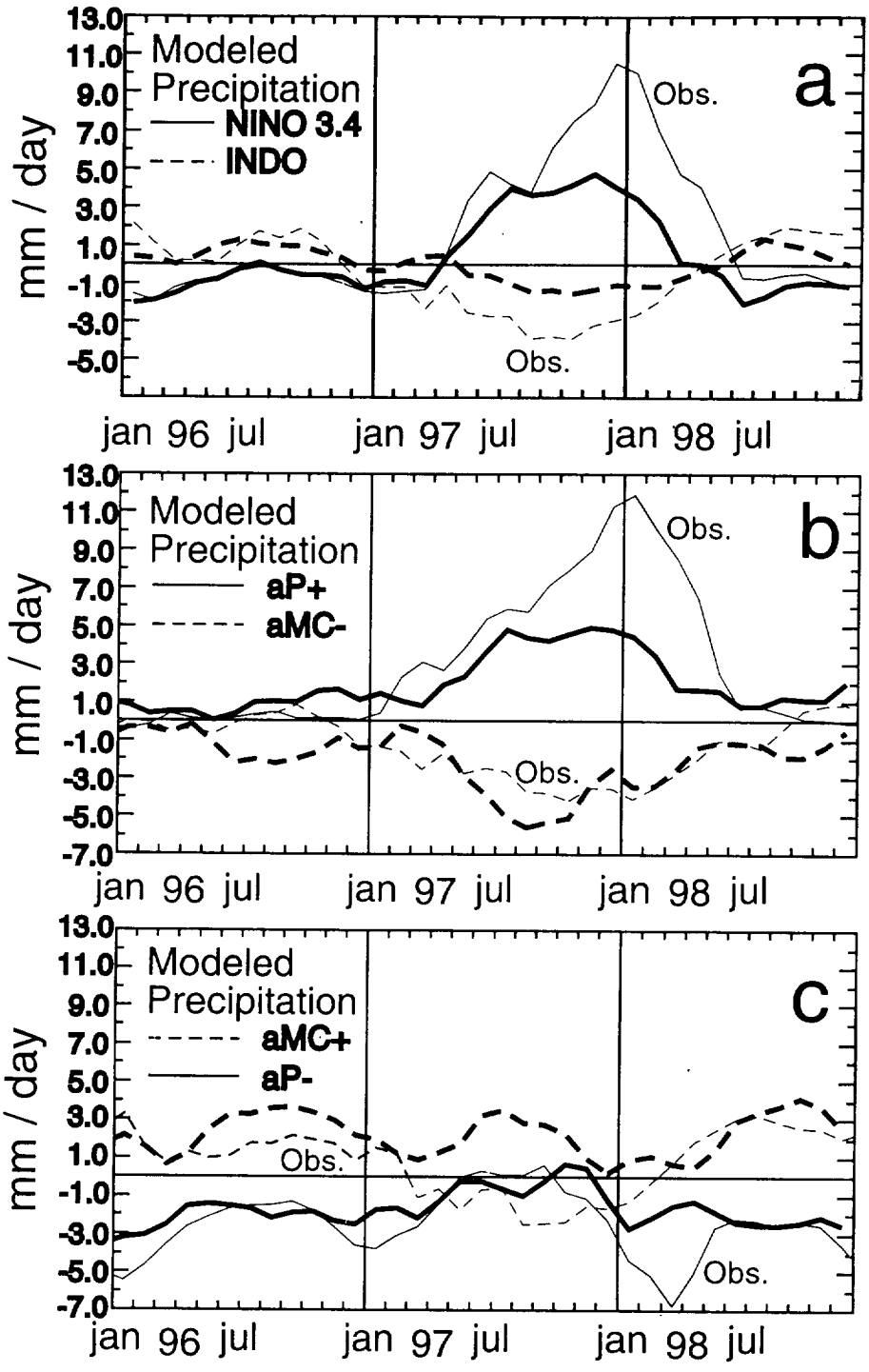
13.0
11.0
9.0
7.0
5.0
3.0
1.0
-1.0
-3.0
-5.0
-7.0
mm / day
Modeled
Precipitation
NINO 3.4
INDO
Obs.
Obs.
a
jan 96 jul
jan 97 jul
jan 98 jul
Modeled
Precipitation
aP+
aMC-
Obs.
Obs.
b
jan 96 jul
jan 97 jul
jan 98 jul
Modeled
Precipitation
aMC+
aP-
Obs.
Obs.
c
jan 96 jul
jan 97 jul
jan 98 jul

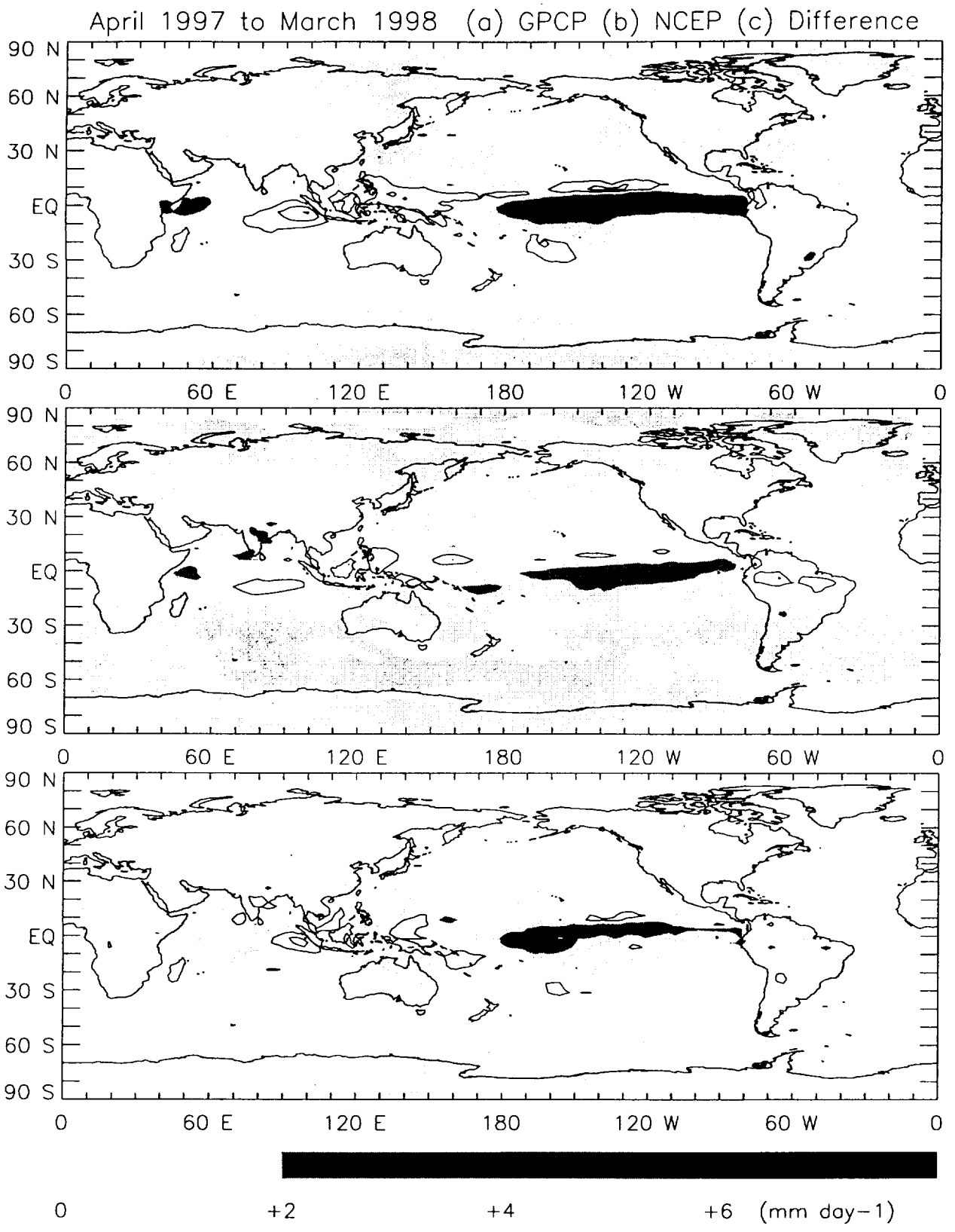
April 1997 to March 1998 (a) GPCP (b) NCEP (c) Difference
90 N
60 N
30 N
EQ
30 S
60 S
90 S
0
60 E
120 E
180
120 W
60 W
0
0
+2
+4
+6 (mm day−1)

References:

Adler RF, Huffman GJ, Bolvin, DT, Curtis S, Nelkin EJ. 2000. Tropical rainfall distributions using TRMM combined with other satellite and raingauge information. *Journal of Applied Meteorology*. accepted.

Bell GD, Halpert MS. 1998. Climate assessment for 1997. *Bulletin of the American Meteorological Society*. 79: S1-S50.

Bell GD, Halpert MS, Ropelewski CF, Kousky VE, Douglas AV, Schnell RC, Gelman ME. 1999. Climate assessment for 1998. *Bulletin of the American Meteorological Society*. 80: S1-S48.

Curtis S, Adler RF. 2000. Precipitation indexes based on patterns of satellite derived precipitation. *Journal of Climate*. in press.

Curtis S, Hastenrath S. 1997. Interannual variability of circulation and climate in the tropical Pacific and Australasia related to the Southern Oscillation. *Journal of the Meteorological Society of Japan*. 75: 819-829.

Harrison DE, Larkin NK. 1998. Seasonal U.S. temperature and precipitation anomalies associated with El Niño: Historical results and comparison with 1997-98. *Geophysical Research Letters*. 25: 3959-3962.

Huffman GJ, Adler RF, Arkin P, Chang A, Ferraro R, Gruber A, Janowiak J, McNab A, Rudolf B, Schneider U. 1997. The Global Precipitation Climatology Project (GPCP) combined precipitation dataset. *Bulletin of the American Meteorological Society.* **78**: 5-20.

Huffman GJ, Adler RF, Morrissey MM, Curtis S, Joyce R, McGavock B, Susskind J. 2000. Global precipitation at one-degree daily resolution from multi-satellite observations. *Journal of Hydrometeorology.* accepted.

Jaksic FM. 1998. The multiple facets of El Niño Southern Oscillation in Chile. *Revista Chilena de Historia Natural.* 71: 121-131.

Janowiak J, Gruber A, Kondragunta CR, Livezey RE, Huffman GJ. 1998. A comparison of the NCEP-NCAR reanalysis precipitation and the GPCP rain gauge-satellite combined dataset with observational error considerations. *Journal of Climate.* 11: 2960-2979.

Jensen MP, Mather JH, Ackerman TP. 1998. Observations of the 1997-98 warm ENSO event at the Manus Island ARM site. *Geophysical Research Letters.* 25: 4517-4520.

Kalnay E, Kanamitsu M, Kistler R, Collins W, Deaven D, Gandin L, Iredell M, Saha S, White G, Woollen J, Zhu Y, Chelliah M, Ebisuzaki W, Higgins W, Janowiak J, Mo KC, Ropelewski C, Wang J, Leetmaa A, Reynolds R, Jenne R, Joseph D. 1996. The NCEP/NCAR 40-year reanalysis project. *Bulletin of the American Meteorological Society*. 77: 437-471.

Kogan FN. 1998. A typical pattern of vegetation conditions in southern Africa during El Niño years detected from AVHRR data using three-channel numerical index. *International Journal of Remote Sensing*. 19: 3689-3695.

Kousky VE ed. 2000. *Climate Diagnostics Bulletin*. Department of Commerce, Camp Springs, MD. 78 pp.

Mc Phadden MJ. 1999. Climate oscillations - Genesis and evolution of the 1997-98 El Niño. *Science*. 283: 950-954.

Montroy DL, Richman MB, Lamb PJ. 1998. Observed nonlinearities of monthly teleconnections between tropical Pacific sea surface temperature anomalies and central and eastern North American precipitation. *Journal of Climate*. 11: 1812-1835.

Mullen C. 1998. Seasonal climate summary southern hemisphere (summer 1997/98): warm event (El Niño) continues. *Australian Meteorological Magazine*. 47: 253-259.

Pavia EG, Badan A. 1998. ENSO modulates rainfall in the Mediterranean Californias. *Geophysical Research Letters.* 25: 3855-3858.

Reynolds RW, Smith TM.1995. A high-resolution global sea surface temperature climatology. *Journal of Climate.* 8: 1571-1583.

Ropelewski CF, Halpert MS. 1987. Global and regional scale precipitation patterns associated with the El Niño/Southern Oscillation. *Monthly Weather Review.* 115: 1606-1626.

Ropelewski, CF, Halpert MS. 1989. Precipitation patterns associated with the high index phase of the Southern Oscillation. *Journal of Climate.* 2: 268-284.

Rudolf B, Hauschild H, Rueth W, Schneider U. 1994. Terrestrial precipitation analysis: operational method and required density of point measurements. *NATO ASI Series.* 126: 173-186.

Susskind J, Piraino P, Rokke L, Iredell L, Mehta A. 1997. Characteristics of the TOVS pathfinder path A dataset. *Bulletin of the American Meteorological Society.* 78: 1449-1472.

Takayabu YN, Iguchi T, Kachi M, Shibata A, Kanzawa H. 1999. An impact of the Madden-Julian oscillation on the abrupt termination of the 1997-98 El Nino. *Nature*. 402: 279-282.

Weare BC. 1983. Interannual variations in net heating at the surface of the tropical Pacific Ocean. *Journal of Physical Oceanography*. 13: 873-885.

Xie P, Arkin PA. 1997. Global precipitation: A 17-year monthly global analysis based on gauge observations, satellite estimates, and numerical model outputs. *Bulletin of the American Meteorological Society*. 78: 2539-2558.

Xie P, Arkin PA. 1998. Global monthly precipitation estimates from satellite-observed outgoing longwave radiation. *Journal of Climate*. 11: 137-164.

Yu L, Rienecker MR. 1998. Evidence of an extratropical atmospheric influence during the onset of the 1997-98 El Niño. *Geophysical Research Letters*. 25: 3537-3540.